

## Research Article

# Molecular Docking, Dynamics Simulations, ADMET, and DFT Calculations: Combined *In Silico* Approach to Screen Natural Inhibitors of 3CL and PL Proteases of SARS-CoV-2

Sugumar Mohanasundaram <sup>1</sup>, Porkodi Karthikeyan,<sup>2</sup> Venkatesan Sampath,<sup>2</sup> M. Anbazhagan,<sup>3</sup> Sundramurthy Venkatesa Prabhu <sup>4,5</sup>, Jamal M. Khaled,<sup>6</sup> and Muthu Thiruvengadam<sup>7</sup>

<sup>1</sup>Department of Biochemistry and Crop Physiology, SRM College of Agricultural Sciences, SRM Institute of Science and Technology, Baburayanpettai, 603201 Maduranthagam Taluk, Chengalpattu District, Tamil Nadu, India

<sup>2</sup>Department of Biochemistry, Sri Sankara Arts and Science College (Autonomous), Enathur, Kanchipuram 631561, Tamil Nadu, India

<sup>3</sup>Department of Environmental Science, Periyar University, Salem, Tamil Nadu, India

<sup>4</sup>Centre for Food Nanotechnology, Department of Food Technology, Faculty of Engineering, Karpagam Academy of Higher Education, Coimbatore 641 021, India

<sup>5</sup>Department of Chemical Engineering, College of Engineering, Addis Ababa Science and Technology University, Ethiopia

<sup>6</sup>Department of Botany and Microbiology, College of Science, King Saud University, Riyadh 11451, Saudi Arabia

<sup>7</sup>Department of Crop Science, College of Sanghuh Life Sciences, Konkuk University, Seoul 05029, Republic of Korea

Correspondence should be addressed to Sundramurthy Venkatesa Prabhu; [venkatesa.prabhu@aastu.edu.et](mailto:venkatesa.prabhu@aastu.edu.et)

Received 19 June 2023; Revised 15 November 2023; Accepted 21 December 2023; Published 16 January 2024

Academic Editor: Shiek Ahmed

Copyright © 2024 Sugumar Mohanasundaram et al. This is an open access article distributed under the Creative Commons Attribution License, which permits unrestricted use, distribution, and reproduction in any medium, provided the original work is properly cited.

Considering natural compounds for the antiviral effect is another opportunity for exploring novel drug candidates for severe acute respiratory syndrome coronavirus 2. The selected natural compounds were interacted using a molecular docking approach. The 3D structures of the main protease and papain-like protease were used for the virtual screening to detect the potent inhibitor against SARS-CoV-2. The top-scored compounds were further analyzed for absorption, digestion, metabolism, excretion, and toxicity properties and density functional theory analysis. Our results indicated that glycyrrhizin exhibited better docking scores of -9.5 kcal/mol with main protease and -9.7 kcal/mol with papain-like protease. Next to glycyrrhizin, rutin showed a better docking score of -9.1 kcal/mol and -9.2 kcal/mol with 3-chymotrypsin-like and papain-like proteases. Violaxanthin and naringin occupied the subsequent position in the docking score table with 3CL and PL proteases, respectively. In addition, the crucial properties like drug likeliness and pharmacokinetics of the compounds were determined. There is no significant toxicity identified.

## 1. Introduction

SARS-CoV-2, the first pandemic of this century, has been detected in 216 countries, with more than 756 million confirmed cases and 68,44,267 deaths as of February 20, 2023. The alteration happening in the genome of this virus resulting in different variants is the biggest challenge among the

scientific community to predict its characteristic features for drug development. The UK found the first mutant variety (called alpha) in September 2020. In May 2020, South Africa found beta, and in November 2020, Brazil found gamma. By October 2020, India had reported the delta variant, and by December 2020, Peru had registered the lambda variant. In January of 2021, Colombia found the Mu species.

The omicron variant has been reported in more than 50 countries (coronavirus disease (COVID-19) pandemic, <https://www.who.int/emergencies/diseases/novel-coronavirus-2019>) [1]. Practical diagnostic approaches have been developed, including RT-PCR, CT imaging, and interleukin-based serological screening [2].

Since the abrupt prerequisite for an effective therapeutic option against SARS-CoV-2 is in the relentless phase of the explosion, evaluating the prevailing antiviral agents for repurposing is obligatory. Many countries conduct *in vivo* and human trials with existing drugs for possible repurposing. Hence, virtual screening of antiviral medications against SARS-CoV-2 will institute a platform for the lead identification process.

Over 250 genome sequences have been deposited into GenBank (GenBank, taxid: 2697049). This  $\beta$ -coronavirus shares an 89% resemblance to the bat coronavirus [3, 4]. A 29 kb size, single-stranded RNA encoding 9,860 amino acids, is present. Since December 2019, researchers have identified several proteins as targets. Main protease, RNA polymerase, and spike protein have attracted outstanding attention owing to their significant role in interactions with the host (human) and the subsequent replication.

Viral proteases are endopeptidases that catalyze the cleavage of viral polyproteins [5]. *Coronaviridae* genomes carry two polyproteins, which get hewed and changed into nonstructural proteins (NSP) by the actions of the 3CL protease and the PL protease [6]. The NSP has a role in viral replication in host cells [7]. As a result, targeting those proteases to mimic the transformation of NSP into biologically functional proteins is worthwhile. The SARS papain-like protease cleaves ISG15 and polyUb [8, 9], whereas 3CL protease is indispensable to the viral life cycle [10].

Food and Drug Administration (FDA) of the USA has not approved any antiviral medicine to treat SARS-CoV-2 except remdesivir under emergency use authorization (EUA). The focus of research has shifted to evaluating the available antiviral drugs. An efficient, naturally occurring drug must be identified and capable of targeting ACE-2 receptors, spike protein, RdRp, or SARS-CoV-2 proteases (<https://www.guidetopharmacology.org/coronavirus.jsp>).

Literature studies indicate that saquinavir, remdesivir, and darunavir and two natural drugs, flavone and coumarin derivatives, were employed to inhibit 3CL protease [11]. Herbal treatment was demonstrated as effective in suppressing infectious diseases during the 2003 SARS outbreak [12]. Significant similarities can be found between SARS-CoV-2 and MERS-CoV [13, 14]. Thus, screening for antiviral compounds in herbals previously used to treat viral pneumonia will expedite the identification of a potential SARS-CoV-2 antiviral drug. In India, *Andrographis paniculata* was widely used to control the dengue outbreak in 2006, following the Ministry of Ayush's recommendations. Traditionally used by the Tamil people of South India, "Nilavembu Kudineer" is an aqueous preparation of *Andrographis paniculata*. It was administered to dengue-infected patients for treatment and to healthy individuals as a prophylactic immune booster. Its antidengue properties have been extensively explored and demonstrated [15]. In India, papaya leaves

were used to treat dengue [16]. An investigation was conducted with 49 naturally occurring metabolites derived from 23 distinct medicinal plant species. Among the total of 49 compounds that were subjected to screening, only 7 exhibited drug-like properties. The study employed molecular docking, dynamics simulation, ADME/T analysis, and DFT analysis to identify naringenin's most promising ligand [17]. Another similar study confirmed that artificially synthesized acyl phloroglucinols showed notable inhibitory potential against SARS-CoV-2 PL protease [17].

Other plants considered include *Azadirachta indica* (Neem), *Eclipta prostrata*, *Carica papaya*, and *Zingiber officinale*, all extensively examined for their antiviral activity [18]. The preceding data concluded that natural antiviral chemicals are critical in mimicking infectious diseases such as SARS, dengue, and chikungunya. As a result, antiviral compounds are chosen for this investigation from the sources listed above.

The objectives of this study were the effective interaction of selected natural compounds with the chosen protein targets by *in silico* docking analysis followed by dynamics simulation analysis and conceptual density functional theory (DFT) computation. Finally, the absorption, digestion, metabolism, excretion, and toxicity (ADMET) properties were investigated to determine their drug-like properties.

## 2. Materials and Methods

**2.1. Retrieval of Protein Receptor.** The 3D structures of 3CL protease (PDB ID: 7C8T) and PL protease (PDB ID: 6WX4) were downloaded from the Protein Data Bank based on the resolution of crystal structure (Figure 1).

**2.2. Retrieval of Ligands.** 3D structures of antiviral compounds (Table 1) such as 6-gingerol, catechin, chlorogenic acid, coumaric acid, caricaxanthin, dasyscyphin C, glycyrrhizin, hyperoside, kaempferol, naringin, nimbaflavone, quercetin, rutin, violaxanthin, zeaxanthin, and zingiberene were downloaded from PubChem.

**2.3. Ligand and Protein Preparation.** The ligand molecules are prepared by energy minimization using ArgusLab software [19]. The energy minimization has been done by the restricted Hartree-Fock (closed-shell). Until attaining the lowest potential energy, all the ligand molecules were energy minimized. The energy-minimized ligands were used for docking studies.

The 3D structures of chosen protein molecules were directly downloaded from PDB (PDB ID: 7C8T and PDB ID: 6WX4) and used for docking. The water molecules and ligand (inhibitor) were removed from the structure, and the essential polar hydrogen was added to the structure using Discovery Studio Visualizer (version 20.1.0.19295) developed by Dassault Systems BIOVIA Corporation. The prepared protein structure was further finalized using an online server of the Centre for Molecular and Biomolecular Informatics, Radboud University, Netherlands (<https://swift.cmbi.umcn.nl/servers/html/index.html>), and then saved for docking in the form of PDB format [20].

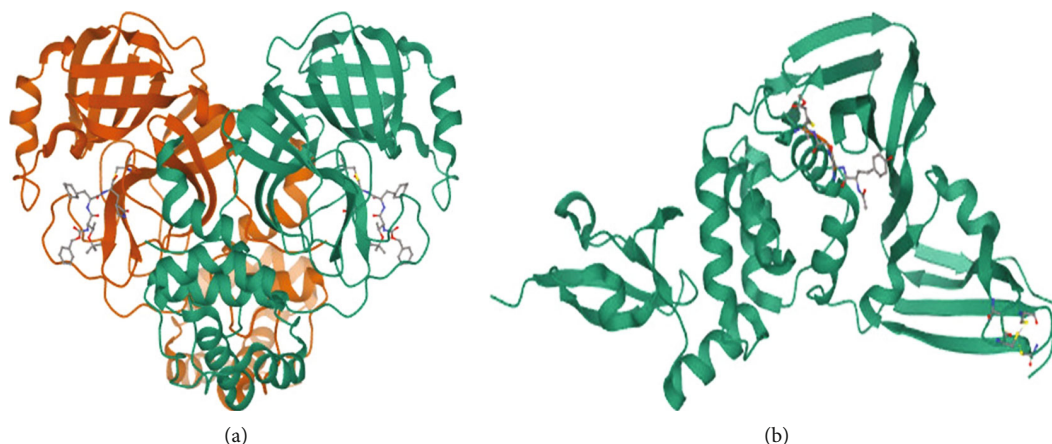


FIGURE 1: (a) 3CL and (b) PL proteases of SARS-CoV-2.

**2.4. Molecular Docking.** PyRx (version 0.8) was used to dock the protein receptors with the selected ligands, and the final output files were obtained as PDBQT files. Individual poses are prepared by a vina split [21]. The amino acids involved in different interactions were observed.

**2.5. Conceptual DFT.** DFT helps analyze a structure by molecular orbital energies [22]. It may help clarify the structure-activity relationship of compounds. DFT calculation will help link biological activities to structure [23]. The Hohenberg and Kohn theorems underpin it [24]. This work used a subset of DFT called conceptual DFT to investigate chemistry using electron density ideas [25]. The electron density of a molecule yields ten separate molecular characteristics, including the electrophilicity index, chemical potential, molecular dipole moment, and electronegativity.

**2.6. Prediction of ADME Properties.** All the ligands used in this study were not approved as drugs by the FDA. As a result, it is critical to understand the drug likelihood of the best ligands targeting both 3CL and PL proteases. The ligands' ADME properties were foreseen by SwissADME (<https://www.swissadme.ch>). The ADME properties were observed [26] for the ligands that showed the best docking score with 3C and papain-like proteases of SARS-CoV-2.

**2.7. Prediction of Toxicity.** The selected best ligands with significant docking scores were subjected to toxicity prediction using the pkCSM (<http://biosig.unimelb.edu.au/pkcsml/>). The canonical SMILES of the target ligands, taken from the PubChem website, were utilized on the pkCSM server under toxicity mode for prediction [27].

**2.8. Molecular Dynamics Simulation.** The glycyrrhizin, rutin, and violaxanthin ligands were simulated using the GROMACS 5.1.2 software and the GROMOS96 54a7 force field. The study mentioned above employed traditional algorithmic techniques and methodologies. The PDBQT files of the docked complexes' main protease and drug molecules were converted to PDB files using Discovery Studio 2020. These PDB data were subsequently refined using Swiss PDB Viewer. GROMACS generated the core protease topol-

ogy file, while PRODRG2 was responsible for creating the topologies of the drug candidates. Topology and data for protein-ligand complexes were generated. Four sodium ions were introduced into a dodecahedron container with a volume of 1 nanometer to preserve electrostatic charge equilibrium, which was subsequently filled with water. The energy was reduced after 1,000 iterations using the steepest descent algorithm. The drug candidates and main protease were later constrained, allowing the solvent to diffuse without restriction. The conditions required for achieving the constant number of particles, volume, and temperature (NVT) and continuous number of particles, pressure, and temperature (NPT) equilibration were as follows. The output analogue coordinates consisted of a total of 500 steps. The computational technique employed in this study was the Particle Mesh Ewald approach, with a cut-off distance of 1.2 nm for the electrostatic interactions. Following the completion of NVT (canonical ensemble) and NPT (isothermal-isobaric ensemble) simulations, production molecular dynamics (MD) runs were conducted at a temperature of 300 K and a pressure of 1 bar, with a time step of 2 femtoseconds. A 20,000-picosecond simulation was performed [20, 28].

### 3. Results

**3.1. Analysis of Docking with 3CL Protease.** To understand the molecular interaction, all compounds were docked with the 3CL protease (PDB ID: 7C8T). Our results indicated that glycyrrhizin had a better docking value of -9.5 kcal/mol and coumaric acid had a lower docking value of -5.3 kcal/mol (Figure 2). Table 2 lists the amino acids of the 3CL protease that form chemical bonds with each ligand. The docking image (Figure 3) of glycyrrhizin with 3C protease revealed seven hydrogen bonds with CYS145, ARG131, LYS137, THR199, LEU287, ASP289, and GLU288 and one electrostatic interaction with LYS137. Compared to glycyrrhizin, rutin (Figure 4) and violaxanthin (Figure 5) demonstrated significant docking scores with 3C protease. Rutin formed six hydrogen bonds and three additional contacts, while violaxanthin formed three hydrophobic connections (Table 2).

TABLE 1: Details of selected ligands.

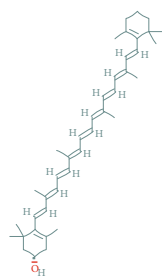
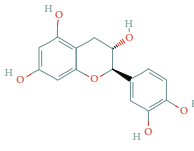
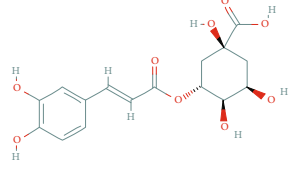
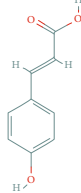
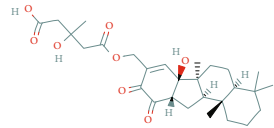
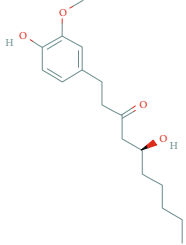
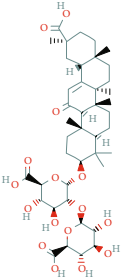
Name	PubChem ID	Molecular weight	Molecular formula	Structure	Antiviral property
Caricaxanthin	44554791	552.9	$C_{40}H_{56}O$		Antidengue
Catechin	9064	290.27	$C_{15}H_{14}O_6$		Anti-influenza, anti-HBV, anti-HSV, antiadenovirus, anti-HIV, antidengue, anti-CHIKV
Chlorogenic acid	1794427	354.31	$C_{16}H_{18}O_9$		Anti-influenza, antihepatitis, anti-HSV
Coumaric acid	637542	164.16	$C_9H_8O_3$		Anti-HIV, anti-influenza, anti-enterovirus, anti-CVA
Dasyscyphin C	11562458	504.6	$C_{28}H_{40}O_8$		Antinodavirus
Gingerol	442793	294.4	$C_{17}H_{26}O_4$		Anti-HCV, anticorona, anti-HRSV
Glycyrrhizin	14982	822.9	$C_{42}H_{62}O_{16}$		Antiherpes, anti-corona-alpha, anti-influenza A, antipolio type I

TABLE 1: Continued.

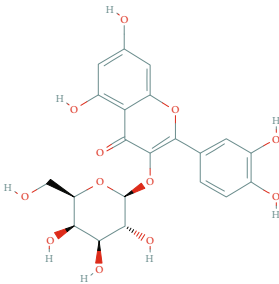
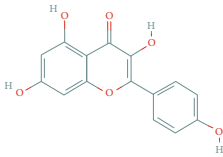
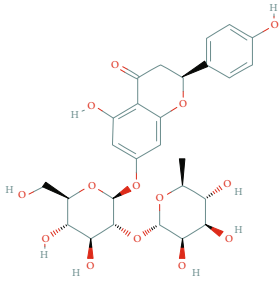
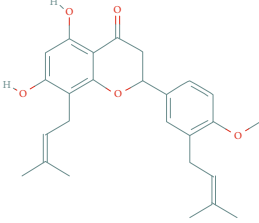
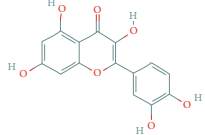
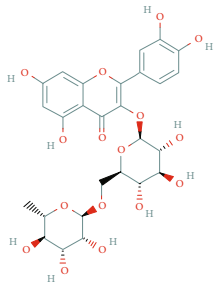
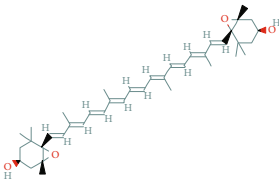
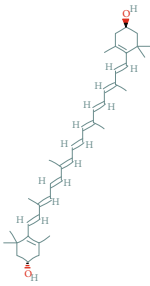
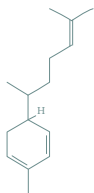
Name	PubChem ID	Molecular weight	Molecular formula	Structure	Antiviral property
Hyperoside	5281643	464.4	$C_{21}H_{20}O_{12}$		Anti-HBV
Kaempferol	5280863	286.24	$C_{15}H_{10}O_6$		Anti-influenza, anti-JEV, anti-HIV
Naringin	442428	580.5	$C_{27}H_{32}O_{14}$		Anti-ZIKV, antidengue
Nimbaflavone	14492795	422.5	$C_{26}H_{30}O_5$		Anti-influenza
Quercetin	5280343	302.23	$C_{15}H_{10}O_7$		Anti-influenza, antiadenovirus, antisyncytial, antirhino
Rutin	5280805	610.5	$C_{27}H_{30}O_{16}$		Anti-influenza, antidengue, antihepatitis

TABLE 1: Continued.

Name	PubChem ID	Molecular weight	Molecular formula	Structure	Antiviral property
Violaxanthin	448438	600.9	C <sub>40</sub> H <sub>56</sub> O <sub>4</sub>		Antidengue
Zeaxanthin	5280899	568.9	C <sub>40</sub> H <sub>56</sub> O <sub>2</sub>		Antidengue
Zingiberene	521253	204.35	C <sub>15</sub> H <sub>24</sub>		Anti-HSV

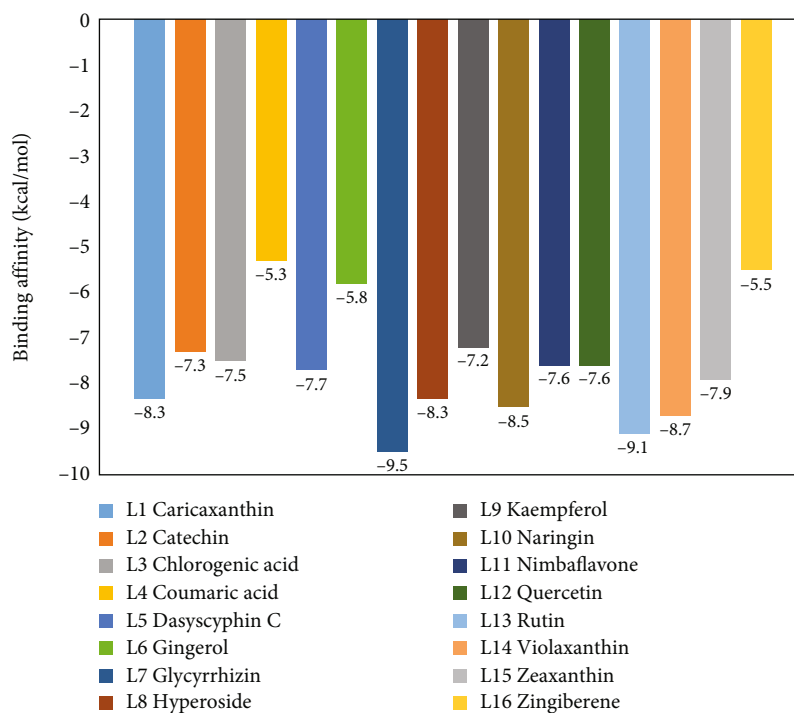


FIGURE 2: Docking score of ligands with 3CL protease.

3.2. *Docking Analysis with PL Protease.* The PL protease (PDB ID: 6WX4) was docked individually with each identified ligand. Glycyrrhizin was discovered with the highest docking value of -9.7kcal/mol (Figure 6). Zingiberene had

the lowest docking value of -4.8kcal/mol. The amino acid details of each ligand's bonding with the protein receptor are listed in Table 3. According to the Discovery Studio Visualizer (Figure 7), glycyrrhizin forms three hydrogen

TABLE 2: The amino acids of 3CL protease involved in bonding.

Ligand	No. of bonds	Details of hydrogen bond		Other interactions	
		Amino acids involved	No. of bonds	Amino acids involved	Bond
Caricaxanthin	—	—	3	TYR154, HIS246, PHE294	Hydrophobic bond
Catechin	1	GLU166	1	CYS145	Pi-sulfur bond
			1	HIS41	Hydrophobic bond
Chlorogenic acid	4	TYR239, ASP289, LEU271, GLU288	2	LEU287, MET276	Hydrophobic bond
Coumaric acid	2	TYR154, GLN306	2	TYR154, PHE294	Hydrophobic bond
Dasyscyphin C	3	LYS137, ASN238, LEU287	—	—	—
Gingerol	3	SER144, ARG188, ASN142	2	HIS41, MET165	Hydrophobic bond
			1	CYS145	Pi-sulfur bond
Glycyrrhizin	7	CYS145, ARG131, LYS137, THR199, LEU287, ASP289, GLU288	1	LYS137	Electrostatic bond
			1	CYS145	Pi-sulfur bond
Hyperoside	6	GLN189, GLN192, MET165, VAL186, LEU141, GLU166	2	HIS41, MET165	Hydrophobic bond
			4	HIS41, LEU141, ASN142, CYS145	Hydrophobic bond
Kaempferol	1	GLU166	4	HIS41, LEU141, ASN142, CYS145	Hydrophobic bond
Naringin	4	GLN110, TYR154, THR111, THR292	—	—	—
Nimbaflavone	2	GLN192, GLN189	5	CYS145, MET49, HIS41, PRO168, MET165	Hydrophobic bond
			2	HIS41, CYS145	Hydrophobic bond
Quercetin	2	PHE140, LEU141	1	CYS145	Pi-sulfur bond
			1	CYS44	Pi-sulfur bond
Rutin	6	SER144, GLN189, THR26, ASP187, GLU166, ASN142	2	HIS41, MET49	Hydrophobic bond
			3	ILE249, TYR154, PHE294	Hydrophobic bond
Violaxanthin	—	—	3	ILE249, TYR154, PHE294	Hydrophobic bond
Zeaxanthin	—	—	2	PRO241, HIS246	Hydrophobic bond
Zingiberene	—	—	1	PHE294	Hydrophobic bond

bonds with PL protease via LEU211, TYR305, and GLY209. Compared to glycyrrhizin, rutin (Figure 8) and naringin (Figure 9) had significant docking scores. Rutin formed four hydrogen bonds and seven other interactions with the PL protease, whereas naringin formed four hydrogen bonds and four other interactions.

**3.3. Prediction of ADME Properties.** The docking investigation revealed that glycyrrhizin and rutin have a better binding affinity for 3CL and PL proteases, respectively. It is worth noting that glycyrrhizin has a high potential for interaction with the 3CL and PL proteases. Compared to glycyrrhizin, rutin has a high potential for interaction with both proteases. ADME properties of the top four ligands are determined by

their docking score for both proteases. As an outcome, glycyrrhizin, rutin, violaxanthin, and naringin were chosen for ADME property prediction using the SwissADME server.

The SwissADME results (Table 4) indicate that none of the ligands can inhibit the cytochrome P450 system, which is a significant finding. All ligands have a negligible level of intestinal absorption rather than none. None of the ligands are capable of passing through the blood-brain barrier. Rutin and naringin are found to be water-soluble, whereas glycyrrhizin and violaxanthin are found to be insoluble and very poorly soluble in water. Compared to the other ligands, glycyrrhizin and violaxanthin do not contain heavy aromatic atoms. To be regarded as a drug-like molecule in ADMET prediction, any molecule must adhere to Lipinski's rule of

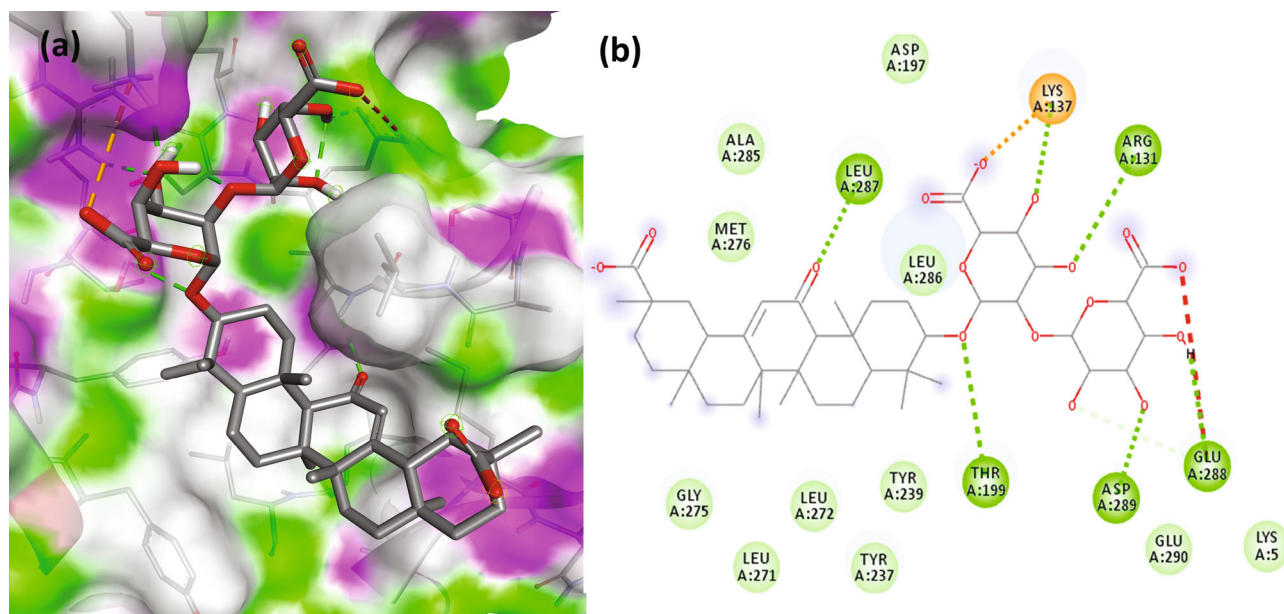


FIGURE 3: 3D (a) and 2D (b) views of glycyrrhizin interaction with 3CL protease.

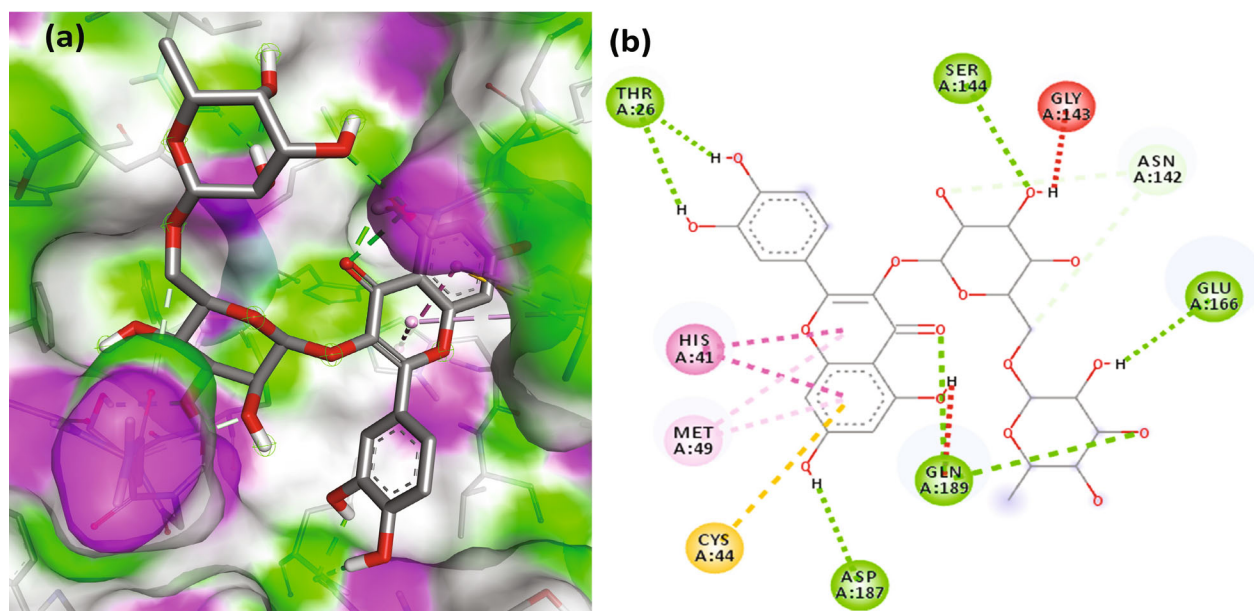


FIGURE 4: 3D (a) and 2D (b) views of rutin interaction with 3CL protease.

5. Here, the final chosen molecules violate some of Lipinski's rules, which must be evaluated before evaluating any ligand as a prospective drug-likeness compound based on its ADME features.

**3.4. Conceptual DFT.** The phytochemicals were optimized using the B3LYP function [29, 30] with a 6-31G (2p, d) basis in Gaussian 16 [31] to determine their molecular properties [32]. The highest occupied molecular orbital (HOMO) energy ( $E_{\text{HOMO}}$ ) and the least unoccupied molecular orbital (LUMO) energy ( $E_{\text{LUMO}}$ ) were calculated, which are critical descriptors that refer to a molecule's ability to donate as well as accept

electrons, correspondingly. We developed and examined maps reflecting the electron density in various locations of the molecules at HOMO and LUMO. The  $E_{\text{HOMO}}$  and  $E_{\text{LUMO}}$  values for the phytochemicals are listed in Table 5.

Table 6 shows the electron density maps of selected phytochemicals' molecular orbitals. We built and evaluated density maps of molecular orbitals. The energy gap ( $E_{\text{gap}}$ ) was determined like  $E = E_{\text{LUMO}} - E_{\text{HOMO}}$ . The energy gap is proportionate to the molecules' reactivity [33]. As a result, with an  $E$  value of -1.22 eV, the rutin protease had the smallest energy gap. Glycyrrhizin, on the other hand, showed the largest, measuring 4.97 eV.



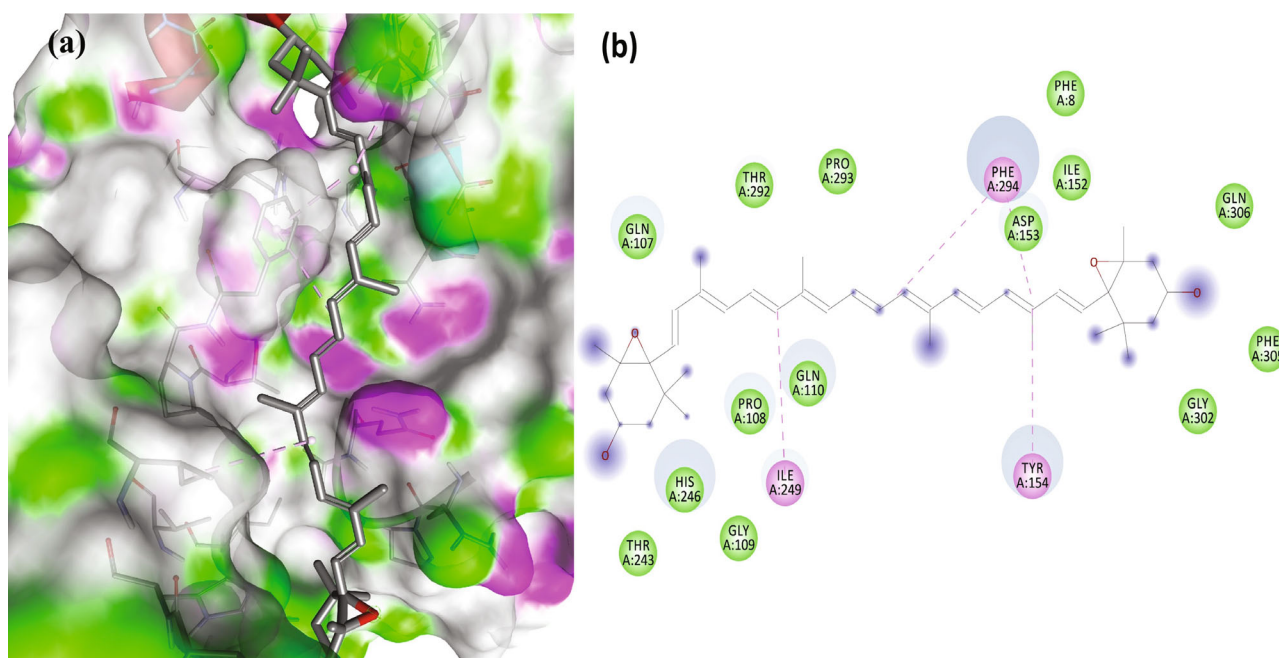


FIGURE 5: 3D (a) and 2D (b) views of violaxanthin interaction with 3CL protease.

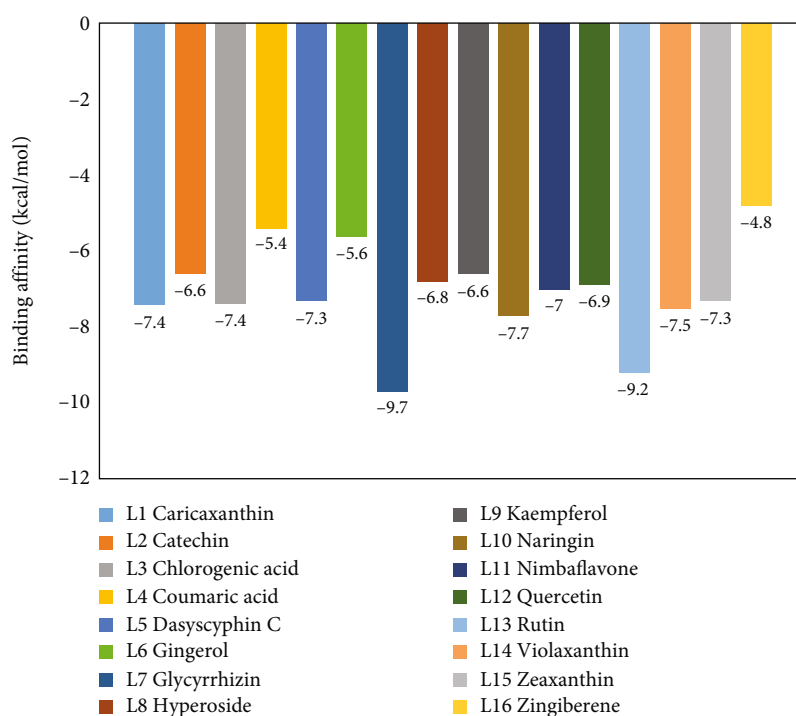


FIGURE 6: Docking scores of ligands with PL protease of SARS-CoV-2.

A molecule's molecular dipole moment can be related to its chemical reactivity [34]. Rutin protease and glycyrrhizin exhibited dipole moments greater than 7.0 Debye. Using predicted  $E_{HOMO}$  and  $E_{LUMO}$  scores, electronegativity and other properties of the ligands were determined. The electron density of a compound is significant because it influ-

ences the electronegativity. If the electronegativity is low, the inhibitory activity will be higher and effective [35]. Glycyrrhizin has the lowest electronegativity value of  $-3.76$  eV, while the rutin protease has a value of  $4.44$  eV. Correlations are found between the values of descriptors for phytochemicals derived using conceptual DFT and the docking analysis.

TABLE 3: Details of amino acids of PL protease involved in bonding.

Name of the ligand	No. of bonds	Details of hydrogen bond		Details of other interactions	
		Amino acids involved	No. of bonds	Amino acids involved	Bond
Caricaxanthin	—	—	5	ARG65, ALA68, PRO77, PRO59, PHE69	Hydrophobic bond
Catechin	6	TYR213, GLU214, LYS254, GLU252, SER212, THR257	1	TYR251	Hydrophobic bond
			1	GLU214	Electrostatic interaction
Chlorogenic acid	5	TYR213, LYS217, TYR305, LYS306, SER212	1	TYR305	Hydrophobic bond
Coumaric acid	2	TYR305, TYR251	1	GLU214	Electrostatic interaction
Dasyscyphin C	5	ARG166, GLN174, SER170, MET206, GLU203	1	TYR207	Hydrophobic bond
Gingerol	4	TYR213, GLU214, TYR305, TYR251	1	GLU214	Electrostatic interaction
			3	TYR305, LYS254, TYR213	Hydrophobic bond
Glycyrrhizin	3	LEU211, TYR305, GLY209	—	—	—
			1	TYR310	Hydrophobic bond
Hyperoside	5	LYS217, GLY256, THR257, GLU307, ASN308	2	GLU214, GLU307	Electrostatic interaction
			1	TYR305	Hydrophobic bond
Kaempferol	3	THR257, GLU252, TYR251	1	GLU214	Electrostatic interaction
			1	GLU214	Electrostatic interaction
Naringin	4	PRO247, THR257, GLU252, LEU211	4	TYR305, LEU211, ALA246, ALA249	Hydrophobic bond
			2	LYS217, GLU214	Electrostatic interaction
Nimbaflavone	1	GLU307	5	THR257, LEU253, VAL303, PHE258, TYR305	Hydrophobic bond
			2	TYR264, PRO248	Hydrophobic bond
Quercetin	1	TYR273	1	GLU307	Electrostatic interaction
			2	TYR264, PRO248	Hydrophobic bond
Rutin	4	LYS217, PHE258, THR257, GLU252	6	LEU253, VAL303, TYR251, PHE258, TYR305, LYS306	Hydrophobic bond
			1	GLU307	Electrostatic interaction
Violaxanthin	1	GLN250	2	TYR251, TYR305	Hydrophobic bond
Zeaxanthin	—	—	2	LYS279, LYS306	Hydrophobic bond
Zingiberene	—	—	4	VAL188, ILE314, PRO316, TYR233	Hydrophobic bond

From this, glycyrrhizin was the highest scoring molecule with huge electronegativity than rutin, which is consistent with the docking analysis.

**3.5. Prediction of Toxicity.** The toxicity of the final selected ligands, glycyrrhizin, rutin, naringin, and violaxanthin, was predicted and analyzed [36]. The results (Table 7) demonstrate unequivocally that none of the four ligands contain AMES toxicity and is neither mutagenic nor carcinogenic. The maximum recommended tolerated dose in humans for all ligands is less than 0.477, which is considered very low. None of the ligands were found to be hepatotoxic or skin-sensitizing. Glycyrrhizin and violaxanthin showed no inhibitory potential on hERG genes encoding for potassium channels. The LD<sub>50</sub> and minnow toxicity values are signifi-

cantly high for all the ligands, which shows that only at very high doses, ligands may tend to cause toxicity ([http://biosig.unimelb.edu.au/pkcsn/static/help/pkcsn\\_theory.pdf](http://biosig.unimelb.edu.au/pkcsn/static/help/pkcsn_theory.pdf)).

**3.6. Molecular Dynamics Simulation.** Following the molecular docking and ADMET prediction analysis, the best three phytochemicals were subjected to research the stability of ligands with 3CL and PL proteases using a molecular dynamics simulation study. Root-mean-square deviation (RMSD), root-mean-square fluctuation (RMSF), and protein-ligand contacts were calculated. Glycyrrhizin, rutin, and violaxanthin molecules show good binding affinity and dug-likeness properties in this docking and ADMET analysis. RMSD, RMSF, Rg, and solvent-accessible surface are shown in Figures 10–12. The average RMSD value of glycyrrhizin, rutin, and violaxanthin

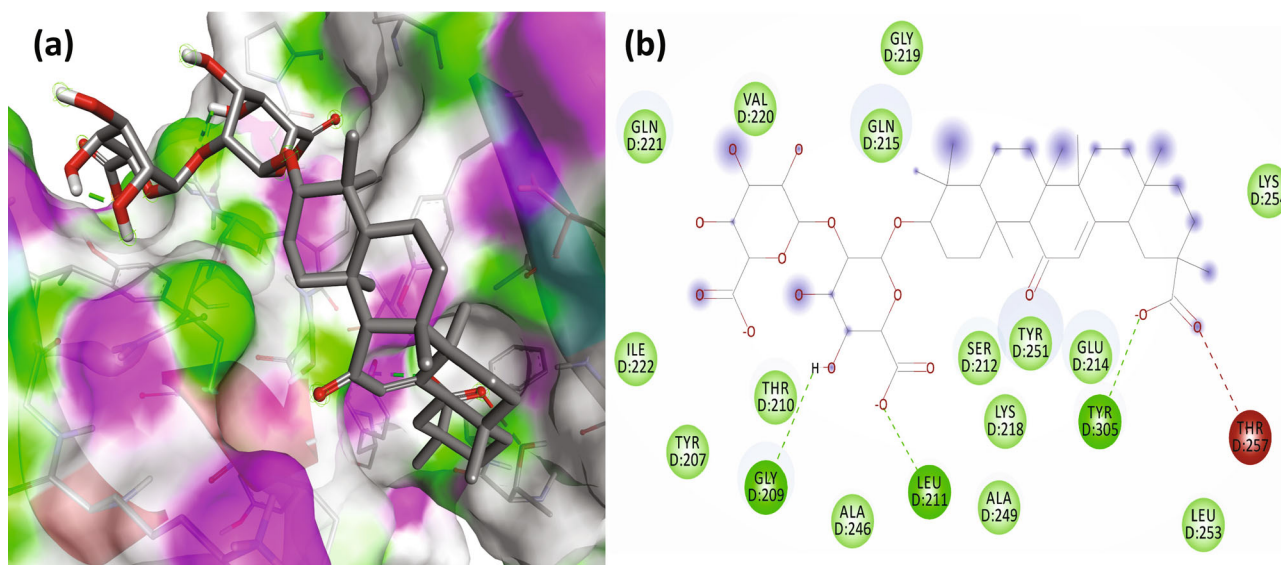


FIGURE 7: 3D (a) and 2D (b) views of glycyrrhizin interaction with PL protease.

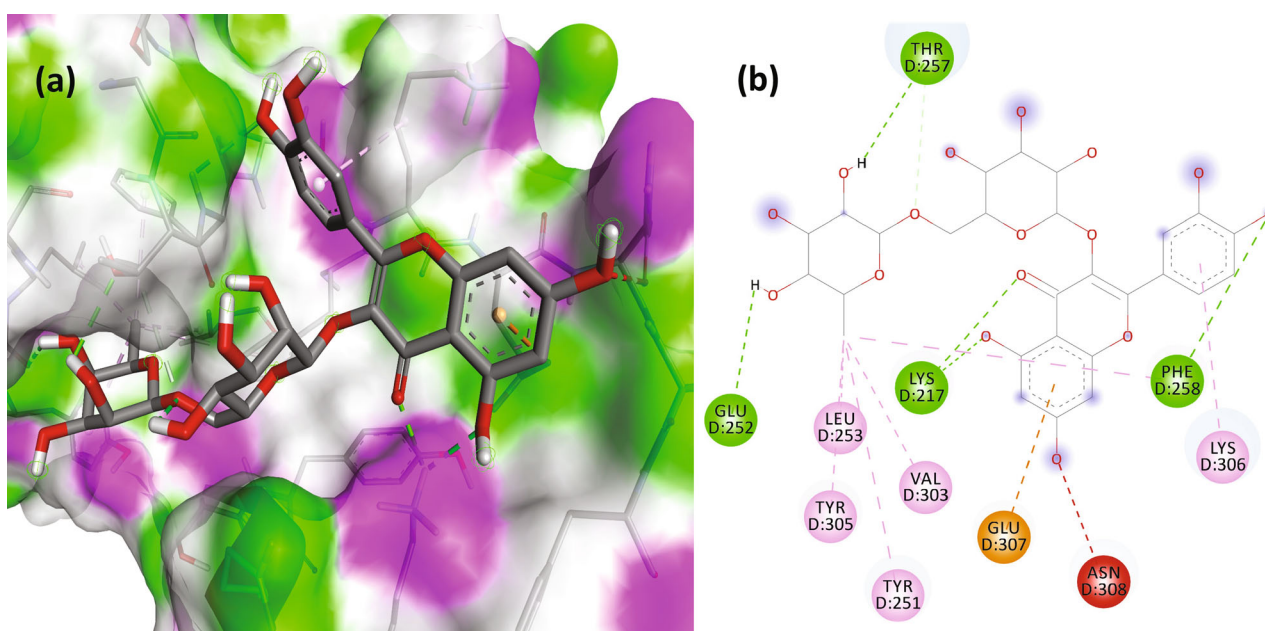


FIGURE 8: 3D (a) and 2D (b) views of rutin interaction with PL protease.

molecules with 3CL and PL proteases shows 0.19 nm, 0.18 nm, and 0.18 nm and 0.2 nm, 0.21 nm, and 0.2 nm, respectively. The stability of the 3CL with glycyrrhizin, rutin, and violaxanthin in radius of gyration (total and around axes) shows at 2.35 Rg (nm) up to 20000 ps.

The results obtained in this investigation are consistent and comparable with the findings reported in the earlier study conducted by Jang et al. [37]. The results demonstrate the stability of the relationship between the natural metabolites and the protein structure. The results obtained for the root-mean-square deviation (RMSD) and root-mean-square fluctuation (RMSF) in our study demonstrate comparable or

superior performance compared to the findings reported in earlier studies. The molecular dynamics simulation conducted for 2000 picoseconds showed encouraging interactions between the protein and the selected metabolites. In the investigation mentioned above, the compounds that were chosen had protein-based root-mean-square deviation (RMSD) values of 0.5, 0.4, and 0.3 nm, respectively (refer to Figure 3(d)). Additionally, their root-mean-square deviation (RMSF) values displayed comparable patterns. Moreover, the in vitro assessment demonstrated that this interaction has a higher degree of stability, indicating inhibitory potential. The findings closely align with our results.

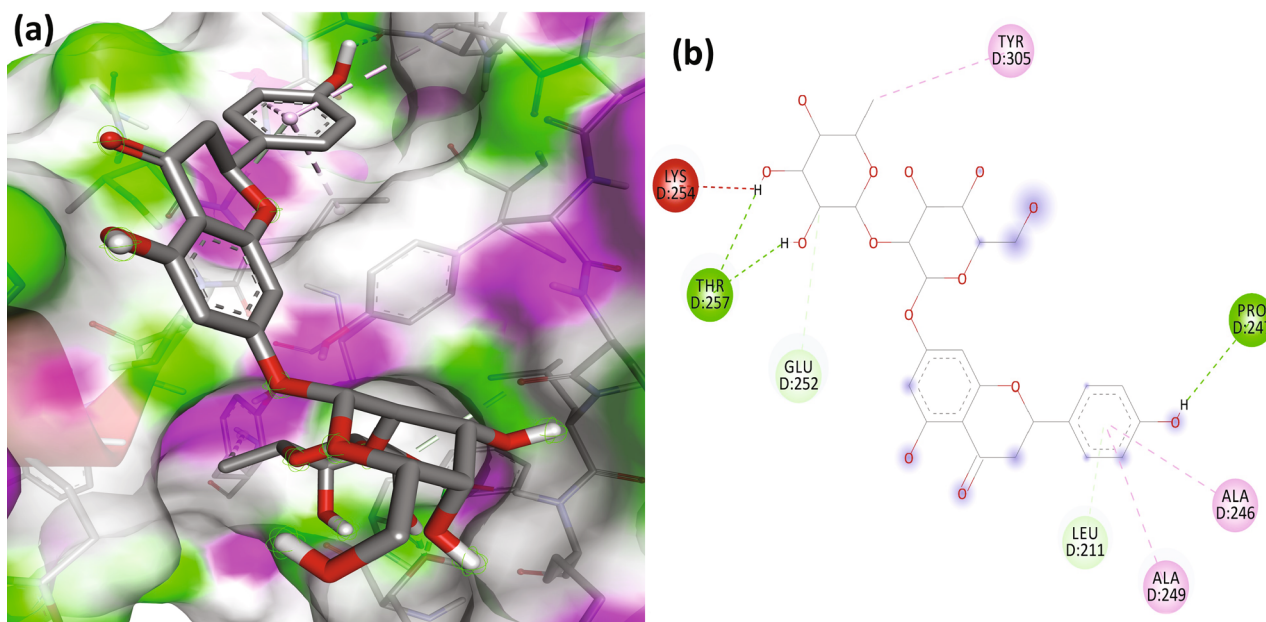


FIGURE 9: 3D (a) and 2D (b) views of naringin interaction with PL protease.

#### 4. Discussions

Virtual screening of the existing antiviral drugs and the naturally available compounds with antiviral properties is essential for the treatment. The widely used drug, remdesivir, is still in trial and is authorized to be used only for emergency management. A recent report [38, 39] stated that combining azithromycin and hydroxychloroquine significantly aided in emergency cases. The inhibition of proteases was observed due to the increase in pH. However, the adverse effects of hydroxychloroquine and azithromycin must be considered, and a side-effect-free alternative is urgently needed [39].

Indian spices are of great importance because of their traditional use as a source of medicine. Many bioactive metabolites with therapeutic applications have been identified [40]. Plants are well characterized and proven for their noteworthy basis of high-value bioactive metabolites, including alkaloids, phenols, flavonoids, coumarins, steroids, and lignans. Plants have widened the window of opportunity to discover natural compounds with therapeutic potential [41–43]. According to a study [44], the plant-derived chemicals carnosol and rosmanol may be employed as therapeutic candidates against SARS-CoV-2. Another study [45] also asserts that three natural substances, ursolic acid, carvacrol, and oleanolic acid, are possible inhibitors.

In this study, four compounds, glycyrrhizin, rutin, violaxanthin, and naringin, were finally chosen from a pool of sixteen compounds based on their docking score.

Glycyrrhizin, the compound with the highest docking score, has been reported to be a moderately potent antiviral agent against HIV and herpes simplex virus [46]. It was recently found as a possible inhibitor of HIV's replicative mechanism [47]. Glycyrrhizin inhibits many viruses, including herpes, corona-alpha, flaviviruses, HIV, Epstein-Barr

virus, influenza A virus, vaccinia, and polio type I viruses [48–53]. Our findings correlated with earlier research, demonstrating a potent 3CL and PL protease inhibitors. The drug is also effective against SARS in vitro studies and may show promise for treating COVID-19 infections. More promising, some derivatives of glycyrrhizin are shown to have a much higher antiviral activity than glycyrrhizin itself [54]. The *in silico* results of this paper are similar to a recent study [55] that has clearly explained the suitability of glycyrrhizin against the 3CL protease of SARS-CoV-2 through in vitro assays, and  $EC_{50}$  value was found to be 0.44 mg/mL.

Additionally, conceptual DFT analyses demonstrate that all molecular characteristics indicate that this compound is a potent inhibitor. The combination of glycyrrhizin and boswellic acid demonstrated efficacy in reducing death rates, accelerating the healing process, and enhancing prognosis or reducing clinical status scores on a 7-point scale. The laboratory findings indicate notable disparities in the serum levels of C-reactive protein (CRP) and the percentage of lymphocytes between the placebo group and the intervention group, providing evidence to support the efficacy of GR+BA in promoting improvement. The combination above has qualities of safety and affordability, rendering it a potential candidate for addressing mild to moderate infections caused by SARS-CoV-2 or its variations associated with COVID-19 [56]. Glycyrrhizin had superior inhibitory effectiveness against SARS-CoV-2 ( $EC_{50} = 300$  mg/L) during the processes of viral adsorption and penetration, in comparison to other antiviral agents such as ribavirin, 6-aziridine, pyrazofurin, and mycophenolic acid, while also demonstrating a higher selectivity index [57].

Rutin has the second-highest docking score. It is a glycosidic derivative of a flavonoid available in natural resources. According to a study [58], the compound's 50% effective concentration ( $EC_{50}$ ) against the cucumber mosaic virus

TABLE 4: ADME properties of the selected ligands.

Property	Glycyrrhizin	Rutin	Naringin	Violaxanthin
Physicochemical properties				
Heavy atoms	58	43	41	44
Aromatic heavy atoms	0	16	12	0
Rotatable bonds	7	6	6	10
H bond acceptors	16	16	14	4
H bond donors	8	10	8	2
TPSA	267.04 Å <sup>2</sup>	269.43 Å <sup>2</sup>	225.06 Å <sup>2</sup>	65.52 Å <sup>2</sup>
Lipophilicity				
Log $P_{o/w}$ (iLOGP)	2.15	2.43	2.38	7.22
Log $P_{o/w}$ (XLOGP3)	2.8	-0.33	-0.44	9.76
Log $P_{o/w}$ (WLOGP)	2.25	-1.69	-1.49	8.97
Log $P_{o/w}$ (MLOGP)	0.02	-3.89	-2.77	5.37
Log $P_{o/w}$ (SILICOS-IT)	0.52	-2.11	-1.64	10.60
Consensus Log $P_{o/w}$	1.55	-1.12	-0.79	8.39
Water solubility				
Log $S$ (ESOL) and class	-6.24 and poorly soluble	-3.3 and soluble	-2.98 and soluble	-9.05 and poorly soluble
Log $S$ (Ali) and class	-8.06 and poorly soluble	-4.87 and moderately soluble	-3.82 and soluble	-11.06 and insoluble
Log $S$ (SILICOS-IT) and class	-1.39 and soluble	-0.29 and soluble	-0.49 and soluble	-5.38 and moderately soluble
Pharmacokinetics				
GI absorption	Low	Low	Low	Low
BBB permeant	No	No	No	No
P-gp substrate	Yes	Yes	Yes	Yes
CYP1A2 inhibitor	No	No	No	No
CYP2C19 inhibitor	No	No	No	No
CYP2C9 inhibitor	No	No	No	No
CYP2D6 inhibitor	No	No	No	No
CYP3A4 inhibitor	No	No	No	No
Log $K_p$ (skin permeation)	-9.33 cm/s	-10.26 cm/s	-10.15 cm/s	-3.04 cm/s
Drug-likeness and violations				
Lipinski's rule of 5 and no. of violations	No and 3	No and 3	No and 3	No and 2
Ghose's filter and no. of violations	No and 3	No and 4	No and 4	No and 4
Veber's filter and no. of violations	No and 1	No and 1	No and 1	Yes and 0
Egan's (Pharmacia) filter and no. of violations	No and 1	No and 1	No and 1	No and 1
Muegge's (Bayer) filter and no. of violations	No and 1	No and 4	No and 3	No and 2
Bioavailability score	0.11	0.17	0.17	0.17
Medicinal chemistry				
PAINS	0 alert	1 alert	0 alert	0 alert
Synthetic accessibility score	8.84	6.52	6.16	7.58

was 394.78 g/mL. A prior work [59] demonstrated that sodium rutin sulfate could be a sulfated rutin analogue that can inhibit HIV-1. Additionally, rutin has been shown [45] to significantly inhibit the avian influenza strain H5N1 in the Madin-Darby canine kidney.

Additionally, there is evidence [60] that rutin significantly inhibits the viral replication cycle during canine distemper virus infection during adsorption and diffusion. The current results of the molecular docking study demonstrate the compound's antiviral activity and suggest that it

TABLE 5: Statistics of molecular descriptors of ligands using DFT.

Compound	Total energy ( $E\gamma$ ) (in eV)	Molecular dipole moment (Debye)	$E_{\text{HOMO}}$ (eV)	$E_{\text{LUMO}}$ (eV)	$E_{\text{gap}}$ (eV)	Absolute hardness ( $\eta$ )	Global softness ( $\sigma$ )	Electronegativity ( $\chi$ )	Chemical potential ( $\mu$ )	Electrophilicity index ( $\omega$ )
Glycyrrhizin	-77321.04	8.97	-6.25	-1.28	4.97	2.48	0.20	-3.76	3.76	2.85
Rutin	-2237.71	7.53	5.05	3.83	-1.22	-0.61	-0.82	4.44	-4.44	-16.19
Naringin	-2101.18	8.0019	-5.97	-1.30	4.67	2.33	0.12	-2.33	2.33	1.16
Violaxanthin	-1858.70	0.4315	-4.87	-1.69	3.18	1.59	0.31	-1.59	1.59	0.79

TABLE 6: Electron density maps of ligands.

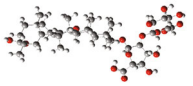
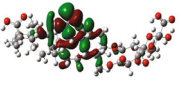
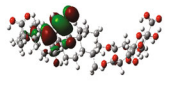
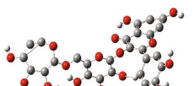
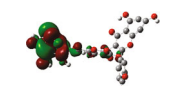
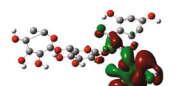
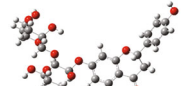
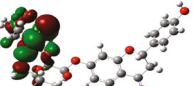
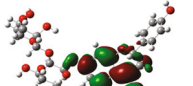
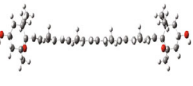
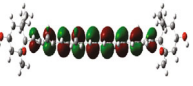
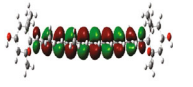
Compound	DFT optimized structure	HOMO	LUMO
Glycyrrhizin			
Rutin			
Naringin			
Violaxanthin			

TABLE 7: Predicted toxicity of the selected ligands.

Property	Glycyrrhizin	Rutin	Naringin	Violaxanthin
AMES toxicity (yes/no)	No	No	No	No
Max. tolerated dose in human (log mg/kg/day)	0.389	0.452	0.43	-0.384
hERG I inhibitor (yes/no)	No	No	No	No
hERG II inhibitor (yes/no)	No	Yes	Yes	No
Oral rat acute toxicity ( $\text{LD}_{50}$ ) (mol/kg)	2.48	2.491	2.495	2.132
Oral rat chronic toxicity (LOAEL) (log mg/kg_bw/day)	5.889	3.673	4.202	2.054
Hepatotoxicity (yes/no)	No	No	No	No
Skin sensitization (yes/no)	No	No	No	No
<i>T. pyriformis</i> toxicity (log $\mu\text{g/L}$ )	0.285	0.285	0.285	0.308
Minnnow toxicity (log mM)	5.591	7.677	6.042	-2.492

may be a significant inhibitor of both 3CL and PL proteases. It has been studied [61] that rutin can inhibit 3CL protease. The findings of the conceptual DFT calculation also indicate that it can be a probable inhibitor next to glycyrrhizin.

Violaxanthin is a naturally occurring orange-coloured xanthophyll pigment found in plants. *In silico* analysis demonstrated a moderate antidengue potential for this compound [62]. There is scant evidence for violaxanthin's antiviral properties; however, there is evidence for its anti-

inflammatory, antiproliferative, and antioxidant properties. Thus, more research and in vitro testing are required to demonstrate its antiviral efficacy.

The fourth ligand with an exceptionally high docking score, naringin, a flavanone 7-O-glycoside, is found in citrus fruits, particularly grapefruits. Naringin was found to have antiadsorption properties against dengue virus—type 2 in a study [63], with an  $\text{IC}_{50}$  of 168.2 g/mL and a corresponding selectivity index of 1.3. Another study [64] reported that

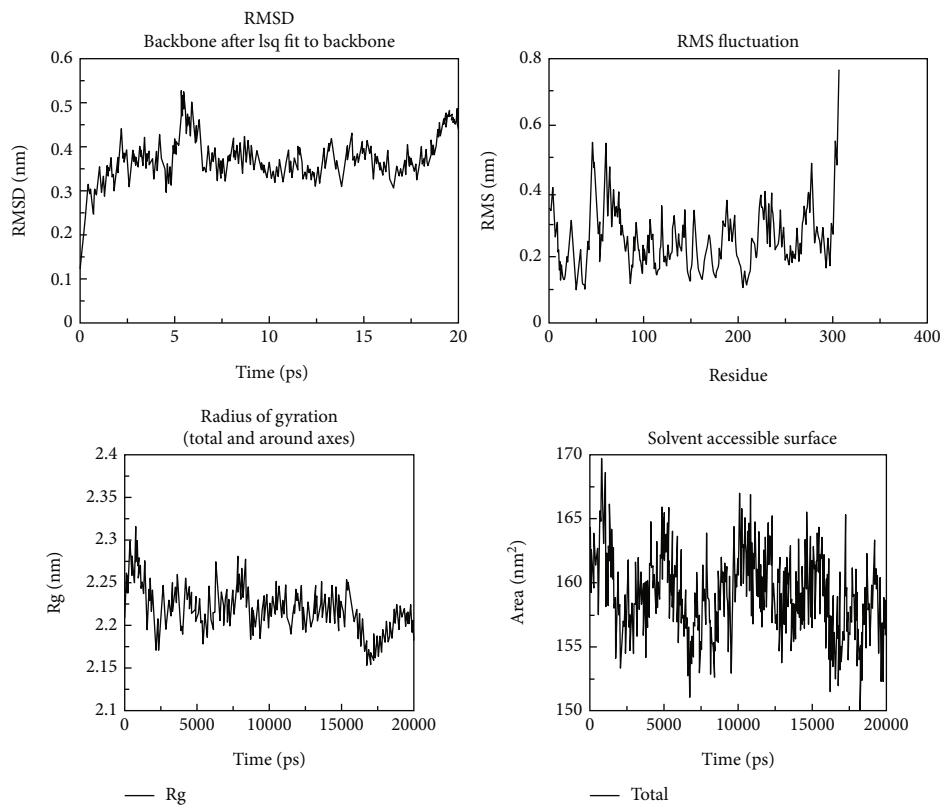


FIGURE 10: RMSD, RMSF, Rg, and solvent-accessible surface analysis of glycyrrhizin main (3CL) protease.

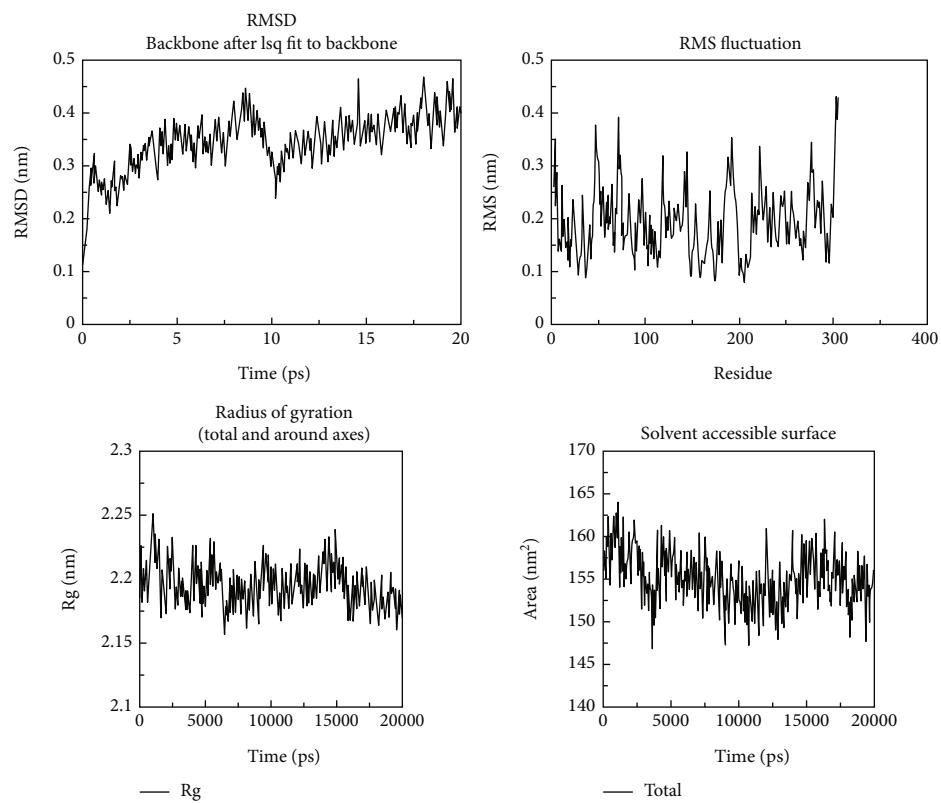


FIGURE 11: RMSD, RMSF, Rg, and solvent-accessible surface analysis of rutin main (3CL) protease.

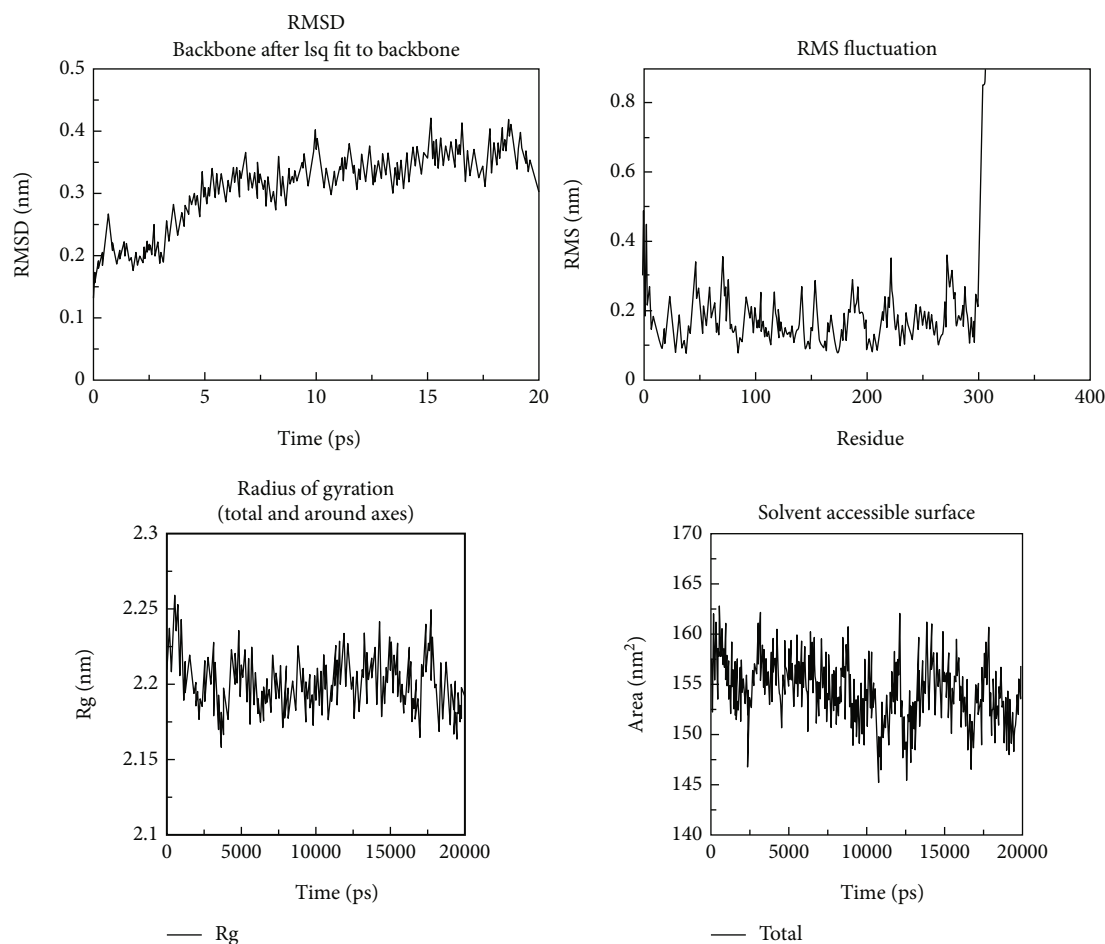


FIGURE 12: RMSD, RMSF, Rg, and solvent-accessible surface analysis of violaxanthin main (3CL) protease.

naringin interacted successfully with the chikungunya virus's nsp2, inhibiting viral replication at the initiation stage. Naringin also suppresses human rotavirus (Wa-1 strain) [65, 66]. The docking research results indicate that it can interact strongly with 3CL and PL proteases. Using conceptual DFT calculations, violaxanthin and naringin are placed third and fourth in potency.

Molecular dynamics simulation validated the conversational stability of glycyrrhizin, rutin, and violaxanthin molecules with the main protease. The RMSD of these ligands showed minor fluctuation with each protein conformation at 20 ns. Also, the binding nature of glycyrrhizin, rutin, and violaxanthin ligands with 3CL did not produce any conformational stability of the protein. Furthermore, the RMSF analysis shows that the best ligands were firmly bound to the active site of the 3CL protein and did not change the loop sections. The gyration radius was also examined to illustrate the protein's structural alterations. Figures 10–12 show the time development of the Rg of 3CL subjected to applied electric fields of various strengths and directions. The value of Rg rises with the power of the applied electric field  $E \leq 0.3$  V/nm. When 1BBL is exposed to electric fields, the importance of Rg becomes increasingly exceptional  $E \geq 0.5$  V/nm as the intensity of the electric field increases due to the protein's extension along the electric field. The protein-ligand

association was stable during MD modelling, with slight backbone changes.

According to the toxicity prediction, glycyrrhizin and violaxanthin exhibited no toxicity with a higher  $LD_{50}$  value. Additionally, rutin and naringin inhibited the hERG II gene. The chosen ligands are prospective antiviral medicines due to their effective interaction with proteases. As per the results of ADME property prediction, glycyrrhizin is the best choice for an antiviral molecule with specific breaches of Lipinski's rule. Additionally, no substantial toxicity was detected using toxicological prediction. Interactions with SARS-CoV-2 proteases *in silico* demonstrate their ability to work against various viruses. While glycyrrhizin, rutin, and naringin all exhibit promising antiviral effects, their drug-likeness violations should not be overlooked when considering them as drug lead compounds. As a result, glycyrrhizin is the best antiviral drug and may be a probable alternative treatment option.

## 5. Conclusion

Repurposing existing medications and utilizing natural antiviral compounds can be the best scientific option until the development of a new drug. The primary target of most viral infections, including HIV, dengue, SARS, influenza,



and n-COVID-19, is a protease. The *in silico* screening of sixteen natural antiviral medicines for their capacity to inhibit the SARS-CoV-2 protease suggests that glycyrrhizin and rutin may be deemed more powerful antiviral agents than others. Additionally, their ADME and toxicology features indicate their potential as anti-SARS-CoV-2 agents. Also, molecular dynamics simulation analysis reveals the strong interaction of top ligands with the protein targets. As a result, additional research and trials are necessary to establish them as antiviral agents.

## Data Availability

The data used to support the findings of this study are included in the article.

## Consent

All authors agree to the publishing of the paper.

## Conflicts of Interest

The authors declare no conflict of interest.

## Authors' Contributions

Sugumar Mohanasundaram was responsible for the methodology and investigation and wrote the original draft. Porkodi Karthikeyan was responsible for the software and supervision and wrote, reviewed, and edited the manuscript. Venkatesan Sampath was responsible for the conceptualization and supervision. Anbazhagan. M was responsible for the methodology and wrote, reviewed, edited, and validated the manuscript. Sundramurthy Venkatesa Prabhu was responsible for the conceptualization and supervision and wrote, reviewed, and edited the manuscript. Jamal M. Khaled was responsible for the funding acquisition and validation. Muthu Thiruvengadam was responsible for the conceptualization and supervision.

## Acknowledgments

The authors extend their appreciation to the Deputyship for Research and Innovation, "Ministry of Education" in Saudi Arabia for funding this research (IFKSUOR3-457-2).

## References

- [1] "Coronavirus disease (COVID-19) pandemic," 2019, <http://www.who.int/emergencies/diseases/novel-coronavirus-2019>.
- [2] A. Sharma, F. I. Ahmad, and S. K. Lal, "COVID-19: a review on the novel coronavirus disease evolution, transmission, detection, control and prevention," *Viruses*, vol. 13, no. 2, p. 202, 2021.
- [3] J. F. W. Chan, K. H. Kok, Z. Zhu et al., "Genomic characterization of the 2019 novel human-pathogenic coronavirus isolated from a patient with atypical pneumonia after visiting Wuhan," *Emerging Microbes & Infections*, vol. 9, no. 1, pp. 221–236, 2020.
- [4] R. Lu, X. Zhao, J. Li et al., "Genomic characterisation and epidemiology of 2019 novel coronavirus: implications for virus origins and receptor binding," *Lancet*, vol. 395, no. 10224, pp. 565–574, 2020.
- [5] J. Konvalinka, H. G. Kräusslich, and B. Müller, "Retroviral proteases and their roles in virion maturation," *Virology*, vol. 479–480, pp. 403–417, 2015.
- [6] R. Hilgenfeld, "From SARS to MERS: crystallographic studies on coronaviral proteases enable antiviral drug design," *The FEBS Journal*, vol. 281, no. 18, pp. 4085–4096, 2014.
- [7] V. Thiel, K. A. Ivanov, A. Putics et al., "Mechanisms and enzymes involved in SARS coronavirus genome expression," *The Journal of General Virology*, vol. 84, no. 9, pp. 2305–2315, 2003.
- [8] V. G. Bhoj and Z. J. Chen, "Ubiquitylation in innate and adaptive immunity," *Nature*, vol. 458, no. 7237, pp. 430–437, 2009.
- [9] M. K. Isaacson and H. L. Ploegh, "Ubiquitination, ubiquitin-like modifiers, and deubiquitination in viral infection," *Cell Host & Microbe*, vol. 5, no. 6, pp. 559–570, 2009.
- [10] P. Mukherjee, F. Shah, P. Desai, and M. Avery, "Inhibitors of SARS-3CLpro: virtual screening, biological evaluation, and molecular dynamics simulation studies," *Journal of Chemical Information and Modeling*, vol. 51, no. 6, pp. 1376–1392, 2011.
- [11] S. A. Khan, K. Zia, S. Ashraf, R. Uddin, and Z. Ul-Haq, "Identification of chymotrypsin-like protease inhibitors of SARS-Cov-2 via integrated computational approach," *Journal of Biomolecular Structure and Dynamics*, vol. 39, no. 7, pp. 2607–2616, 2020.
- [12] Z. Chen and T. Nakamura, "Statistical evidence for the usefulness of Chinese medicine in the treatment of SARS," *Phytotherapy Research*, vol. 18, no. 7, pp. 592–594, 2004.
- [13] H. Y. Tian, "2019-nCoV: new challenges from coronavirus," *Chinese with Abstract in English*, vol. 54, p. E001, 2020.
- [14] P. Zhou, X. L. Yang, X. G. Wang et al., "A pneumonia outbreak associated with a new coronavirus of probable bat origin," *Nature*, vol. 579, no. 7798, pp. 270–273, 2020.
- [15] K. Krishnasamy, S. Ramalingam, S. Karupannan et al., "Anti-dengue activity of *Andrographis paniculata* extracts and quantification of dengue viral inhibition by SYBR green reverse transcription polymerase chain reaction," *An International Quarterly Journal of Research in Ayurveda*, vol. 39, no. 2, pp. 87–91, 2018.
- [16] P. Senthilvel, P. Lavanya, K. M. Kumar et al., "Flavonoid from *Carica papaya* inhibits NS2B-NS3 protease and prevents dengue 2 viral assembly," *Bioinformation*, vol. 9, no. 18, pp. 889–895, 2013.
- [17] W. E. Prasetyo, H. Purnomo, M. Sadrini, F. R. Wibowo, M. Firdaus, and T. Kusumaningsih, "Identification of potential bioactive natural compounds from Indonesian medicinal plants against 3-chymotrypsin-like protease (3CLpro) of SARS-CoV-2: molecular docking, ADME/T, molecular dynamic simulations, and DFT analysis," *Journal of Biomolecular Structure and Dynamics*, vol. 41, no. 10, pp. 4467–4484, 2023.
- [18] B. N. Dhawan, "Antiviral activity of Indian plants," *Proceedings of the National Academy of Sciences, India Section B*, vol. 82, no. 1, pp. 209–224, 2012.
- [19] M. A. Thompson, "Molecular docking using ArgusLab, an efficient shape-based search algorithm and AScore scoring function," in *Proceedings of the ACS Meeting*, Philadelphia, Pa, USA, 2004172: CINF 42.
- [20] S. Sivakumar, S. Mohanasundaram, N. Rangarajan, V. Sampath, and M. V. Dass Prakash, "In silico prediction of interactions and molecular dynamics simulation analysis of Mpro of severe acute respiratory syndrome caused by novel

- coronavirus 2 with the FDA-approved nonprotein antiviral drugs," *Journal of Applied Pharmaceutical Science*, vol. 12, no. 5, pp. 104–119, 2022.
- [21] R. T. Kroemer, "Structure-based drug design: docking and scoring," *Current Protein & Peptide Science*, vol. 8, no. 4, pp. 312–328, 2007.
- [22] P. Geerlings, E. Chamorro, P. K. Chattaraj et al., "Conceptual density functional theory: status, prospects, issues," *Theoretical Chemistry Accounts*, vol. 139, no. 2, p. 36, 2020.
- [23] S. K. Nagarajan, S. Babu, H. Sohn, P. Devaraju, and T. Madhavan, "Toward a better understanding of the interaction between somatostatin receptor 2 and its ligands: a structural characterization study using molecular dynamics and conceptual density functional theory," *Journal of Biomolecular Structure and Dynamics*, vol. 37, no. 12, pp. 3081–3102, 2019.
- [24] P. Hohenberg and W. Kohn, "Inhomogeneous electron gas," *Physics Review*, vol. 136, no. 3B, pp. B864–B871, 1964.
- [25] L. R. Domingo, M. Ríos-Gutiérrez, and P. Pérez, "Applications of the conceptual density functional theory indices to organic chemistry reactivity," *Molecules*, vol. 21, no. 6, p. 748, 2016.
- [26] A. Daina, O. Michielin, and V. Zoete, "SwissADME: a free web tool to evaluate pharmacokinetics, drug-likeness and medicinal chemistry friendliness of small molecules," *Scientific Reports*, vol. 7, no. 1, article 42717, 2017.
- [27] D. E. Pires, T. L. Blundell, and D. B. Ascher, "PkCSM: predicting small-molecule pharmacokinetic and toxicity properties using graph-based signatures," *Journal of Medicinal Chemistry*, vol. 58, no. 9, pp. 4066–4072, 2015.
- [28] M. J. Abraham, T. Murtola, R. Schulz et al., "GROMACS: high performance molecular simulations through multi-level parallelism from laptops to supercomputers," *Software X*, vol. 1–2, pp. 19–25, 2015.
- [29] A. Becke, "Density-functional exchange-energy approximation with correct asymptotic behavior," *Physical Review A*, vol. 38, no. 6, pp. 3098–3100, 1988.
- [30] C. Lee, W. Yang, and R. Parr, "Development of the Colle-Salvetti correlation-energy formula into a functional of the electron density," *Physical Review B*, vol. 37, no. 2, pp. 785–789, 1988.
- [31] M. Frisch, G. Trucks, H. Schlegel et al., *Gaussian 16 (version revision B.01) [Linux]*, Gaussian, Inc., Wallingford CT, 2016.
- [32] K. Fukui, "The role of frontier orbitals in chemical reactions (Nobel lecture)," *Angewandte Chemie International Edition in English*, vol. 21, no. 11, pp. 801–809, 1982.
- [33] R. Bostan, S. Varvara, L. Găină, and L. M. Mureșan, "Evaluation of some phenothiazine derivatives as corrosion inhibitors for bronze in weakly acidic solution," *Corrosion Science*, vol. 63, pp. 275–286, 2012.
- [34] B. Mert, M. Erman Mert, G. Kardas, and B. Yazıcı, "Experimental and theoretical investigation of 3-amino-1,2,4-triazole-5-thiol as a corrosion inhibitor for carbon steel in HCl medium," *Corrosion Science*, vol. 53, no. 12, pp. 4265–4272, 2011.
- [35] C. Zhan, J. Nichols, and D. Dixon, "Ionization potential, electron affinity, electronegativity, hardness, and electron excitation energy: molecular properties from density functional theory orbital energies," *The Journal of Physical Chemistry*, vol. 107, no. 20, pp. 4184–4195, 2003.
- [36] M. Wang, R. Cao, L. Zhang et al., "Remdesivir and chloroquine effectively inhibit the recently emerged novel coronavirus (2019-nCoV) in vitro," *Cell Research*, vol. 30, no. 3, pp. 269–271, 2020.
- [37] J. H. Kim, Y.-I. Park, M. Hur et al., "Inhibition by components of Glycyrrhiza uralensis of 3CLpro and HCoV-OC43 proliferation," *Journal of Enzyme Inhibition and Medicinal Chemistry*, vol. 38, no. 1, p. 1, 2023.
- [38] Y. K. Bokam, C. Guntupalli, S. N. K. R. Gudhanti et al., "Importance of pharmacists as a front line warrior in improving medication compliance in Covid-19 patients," *Indian Journal of Pharmaceutical Sciences*, vol. 83, no. 2, pp. 398–401, 2021.
- [39] S. K. Enmozhi, K. Raja, I. Sebastine, and J. Joseph, "Andrographolide as a potential inhibitor of SARS-CoV-2 main protease: an in silico approach," *Journal of Biomolecular Structure and Dynamics*, vol. 39, no. 9, pp. 1–7, 2020.
- [40] K. R. A. Sachan, S. Kumar, K. Kumari, and D. Singh, "Medicinal uses of our spices used in our traditional culture," *Journal of Medicinal Plant Studies*, vol. 6, no. 3, pp. 116–122, 2018.
- [41] B. Jee, S. Kumar, R. Yadav, Y. Singh, A. Kumar, and M. Sharma, "Ursolic acid and carvacrol may be potential inhibitors of dormancy protein small heat shock protein 16.3 of Mycobacterium tuberculosis," *Journal of Biomolecular Structure and Dynamics*, vol. 36, no. 13, pp. 3434–3443, 2018.
- [42] A. Kumar, R. Kumar, M. Sharma, U. Kumar, M. N. P. Gajula, and K. P. Singh, "Uttarakhand medicinal plants database (UMPDB): a platform for exploring genomic, chemical, and traditional knowledge," *Data (Data)*, vol. 3, no. 1, p. 7, 2018.
- [43] S. S. Panchangam, M. Vahedi, M. J. Megha et al., "Saffron'omics': the challenges of integrating omic technologies," *Avicenna Journal of Phytomedicine*, vol. 6, no. 6, pp. 604–620, 2016.
- [44] D. K. Umesh, C. Selvaraj, S. K. Singh, and V. K. Dubey, "Identification of new anti-nCoV drug chemical compounds from Indian spices exploiting SARS-CoV-2 main protease as target," *Journal of Biomolecular Structure and Dynamics*, vol. 39, no. 9, pp. 1–9, 2020.
- [45] A. Kumar, G. Choudhir, S. K. Shukla et al., "Identification of phytochemical inhibitors against main protease of COVID-19 using molecular modeling approaches," *Journal of Biomolecular Structure and Dynamics*, vol. 39, no. 10, pp. 3760–3770, 2021.
- [46] G. Williams, C. Leclercq, and A. G. A. C. Knaap, *WHO Food Additives Series 54: Safety and Evaluation of Certain Food Additives*, WHO, Geneva, 2006.
- [47] M. Ito, A. Sato, K. Hirabayashi et al., "Mechanism of inhibitory effect of glycyrrhizin on replication of human immunodeficiency virus (HIV)," *Antiviral Research*, vol. 10, no. 6, pp. 289–298, 1988.
- [48] J. Cinatl, B. Morgenstern, G. Bauer, P. Chandra, H. Rabenau, and H. W. Doerr, "Glycyrrhizin, an active component of liquorice roots, and replication of SARS-associated coronavirus," *Lancet*, vol. 361, no. 9374, pp. 2045–2046, 2003.
- [49] J. M. Crance, N. Scaramozzino, A. Jouan, and D. Garin, "Interferon, ribavirin, 6-azauridine and glycyrrhizin: antiviral compounds active against pathogenic flaviviruses," *Antiviral Research*, vol. 58, no. 1, pp. 73–79, 2003.
- [50] S. Harada, "The broad antiviral agent glycyrrhizin directly modulates the fluidity of plasma membrane and HIV-1 envelope," *The Biochemical Journal*, vol. 392, no. 1, pp. 191–199, 2005.
- [51] T. Hattori, S. Ikematsu, A. Koito et al., "Preliminary evidence for inhibitory effect of glycyrrhizin on HIV replication in patients with AIDS," *Antiviral Research*, vol. 11, no. 5–6, pp. 255–261, 1989.

- [52] G. Lampis, D. Deidda, M. Pinza, and R. Pompei, "Enhancement of anti-herpetic activity of glycyrrhizic acid by physiological proteins," *Antiviral Chemistry and Chemotherapy*, vol. 12, no. 2, pp. 125–131, 2001.
- [53] J. C. Lin, "Mechanism of action of glycyrrhizic acid in inhibition of Epstein-Barr virus replication in vitro," *Antiviral Research*, vol. 59, no. 1, pp. 41–47, 2003.
- [54] H. Al-Kamel and O. Grundmann, "Glycyrrhizin as a potential treatment for the novel coronavirus (COVID-19)," *Mini-Reviews in Medicinal Chemistry*, vol. 21, no. 16, pp. 2204–2208, 2021.
- [55] L. van de Sand, M. Bormann, M. Alt et al., "Glycyrrhizin effectively inhibits SARS-CoV-2 replication by inhibiting the viral main protease," *Viruses*, vol. 13, no. 4, p. 609, 2021.
- [56] A. A. Gomaa, Y. A. Abdel-Wadood, and M. A. Gomaa, "Glycyrrhizin and boswellic acids, the golden nutraceuticals: multitargeting for treatment of mild-moderate COVID-19 and prevention of post-COVID cognitive impairment," *Inflammopharmacology*, vol. 30, no. 6, pp. 1977–1992, 2022.
- [57] S. Banerjee, S. K. Baidya, N. Adhikari, B. Ghosh, and T. Jha, "Glycyrrhizin as a promising kryptonite against SARS-CoV-2: clinical, experimental, and theoretical evidences," *Journal of Molecular Structure*, vol. 1275, article 134642, 2023.
- [58] H. Yu, Y. Ding, D. Xie et al., "Design, synthesis, and antiviral activity of novel rutin derivatives containing 1, 4-pentadien-3-one moiety," *European Journal of Medicinal Chemistry*, vol. 92, pp. 732–737, 2015.
- [59] J. Tao, Q. Hu, J. Yang et al., "In vitro anti-HIV and -HSV activity and safety of sodium rutin sulfate as a microbicide candidate," *Antiviral Research*, vol. 75, no. 3, pp. 227–233, 2007.
- [60] A. K. Ibrahim, A. I. Youssef, A. S. Arafa, and S. A. Ahmed, "Anti-H5N1 virus flavonoids from *Capparis sinaica* Veill," *Natural Product Research*, vol. 27, no. 22, pp. 2149–2153, 2013.
- [61] B. Rizzuti, F. Grande, F. Conforti et al., "Rutin is a low micromolar inhibitor of SARS-CoV-2 main protease 3CLpro: implications for drug design of quercetin analogs," *Biomedicine*, vol. 9, no. 4, p. 375, 2021.
- [62] O. V. Carvalho, C. V. Botelho, C. G. Ferreira et al., "In vitro inhibition of canine distemper virus by flavonoids and phenolic acids: implications of structural differences for antiviral design," *Research in Veterinary Science*, vol. 95, no. 2, pp. 717–724, 2013.
- [63] N. Radhakrishnan, K. W. Lam, and M. E. Norhaizan, "Molecular docking analysis of *Carica papaya* Linn constituents as antiviral agent," *International Food Research Journal*, vol. 24, no. 4, pp. 1819–1825, 2017.
- [64] K. Zandi, B. Teoh, S. Sam, P. F. Wong, M. R. Mustafa, and S. AbuBakar, "Antiviral activity of four types of bioflavonoid against dengue virus type-2," *Virology Journal*, vol. 8, no. 1, p. 560, 2011.
- [65] P. K. Tripathi, J. Singh, N. Gaurav, D. K. Garg, and A. K. Patel, "In-silico and biophysical investigation of biomolecular interaction between naringin and nsP2 of the chikungunya virus," *International Journal of Biological Macromolecules*, vol. 160, pp. 1061–1066, 2020.
- [66] L. A. Savi, T. Caon, A. P. de Oliveira et al., "Evaluation of anti-rotavirus activity of flavonoids," *Fitoterapia*, vol. 81, no. 8, pp. 1142–1146, 2010.